Experimental study of the equilibria of cesium potassium antimonides with alkali vapours

B. Tanguy, J. M. Barois* and M. Onillon
Laboratoire de Chimie du Solide du CNRS, Université de Bordeaux I, 351, cours de la Libération, 33405 Talence Cedex (France)

(Received January 8, 1991; accepted February 18, 1991)

Abstract

The equilibria between $(Cs_{1-x}K_x)_3Sb$ and alkali vapours have been studied experimentally at 200 °C. The phases synthesized by gas-solid reaction have been compared to those obtained by solid state reaction. The results have been interpreted thermodynamically. They can provide guidance for the manufacture of photoemissive layers.

Introduction

Partially substituting cesium by potassium in the compound Cs_3Sb is a way to improve its photoemissive properties [1]. Alkali antimonides are widely used for manufacturing photocathodes and must then be synthesized *in situ* as thin or semi-thick layers. In practice, antimony is vapour deposited on the glass substrate, then reacted with alkali vapours. Indeed, the composition of the phases obtained depends strongly on the conditions in which the vapour-solid reaction occurs.

The crystal structure of Cs_3Sb is an anti BiF_3 type [2–3] and that of K_3Sb is an Na_3As type [4]. Cubic solid solutions $(Cs_{1-x}K_x)_3Sb$ can be synthesized by direct reaction between the two antimonides in a sealed reactor at 200 °C [5]. When $x=2/3$. *i.e.* for the composition K_2CsSb, X-ray diffraction studies [5] indicate that an ordering occurs for the alkali elements: the cesium ions are then localized in the (b) sites of the Fm3m space group whereas the potassium ions lie in the (c) sites (Fig. 1).

The ordered phase K_2CsSb is characterized by a photoemission threshold close to that of Cs_3Sb. However, for wavelengths close to 400 nm, its quantum yield is higher than that of the other terms of the solid solution and of all the other alkali antimonides [1, 3]. Furthermore, its thermionic emissivity is extremely weak at room temperature, which is not the case for Cs_3Sb. As for K_3Sb, its quantum yield is poor, like that of other antimonides with the Na_3As structure [1].

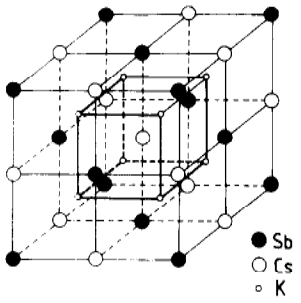

Fig. 1. Crystal structure of CsK_2Sb [5].

Monoalkali antimonides can be either line compounds, such as K_3Sb, or likely to show a slight departure from stoichiometry as shown in one of our previous studies for $\simeq Cs_3Sb$ [7]. The situation is of course different for bialkali antimonides for which the ratio of the two alkali metals can be broadly varied, with subsequent changes in the photoemissive properties.

Industrial bialkali antimonide layers are manufactured according to a process proposed by Sommer [1]: a layer of antimony is reacted with the two alkali vapours successively, starting with the most volatile one. The process implies a substitution of the first metal by the second in the antimonide which is formed initially. Indeed, this substitution is dynamic and the risk is not to reach, or to go beyond, the optimum composition.

In order to determine the conditions for optimum reproducibility in the manufacturing of bialkali antimonides, we have studied the equilibria be-

*Present address: RTC Compelec, Brive la Gaillarde, F-1906, France.

0254-0584/91/$3.50
© 1991 — Elsevier Sequoia, Lausanne

tween $(Cs_{1-x}K_x)_3Sb$ phases and various mixtures of cesium and potassium vapours. All syntheses were carried out at 200 °C which corresponds to industrial practice.

Experimental

The phases $(Cs_{1-x}K_x)_3Sb$ were synthesized by the action of bialkali vapours, generated from a liquid (Cs-K) alloy at temperature T′, on pure solid antimony held in a reactor at temperature $T'' > T'$ in order to avoid distillation. Applying the phase rule to the reactor at T″, where the chemical potentials of both alkali elements are imposed by the composition of the mother alloy and the generator temperature T′, indicates that no more than one condensed phase and with definite composition, can be synthesized in such conditions. By varying the mother alloy composition, and eventually the generator temperature, it is possible to explore the whole composition domain of the $(Cs_{1-x}K_x)_3Sb$ phase.

The apparatus that we used is shown on Fig. 2. Since alkali metals and their antimonides are very sensitive to oxidation, the reactor was outgassed for 12 h under vacuum, charged in a purified argon atmosphere (impurities < 12 ppm) and sealed under vacuum. After the reaction (trial and error showed that 200 h were necessary for the complete combination of the ≃150 mg of powdered antimony used) the reactor was opened in the purified argon atmosphere.

Three couples of temperatures T′ and T″ were used in the study, namely:

set up A	T′ = 100 °C	T″ = 200 °C
B	T′ = 130 °C	″
C	T′ = 180 °C	″

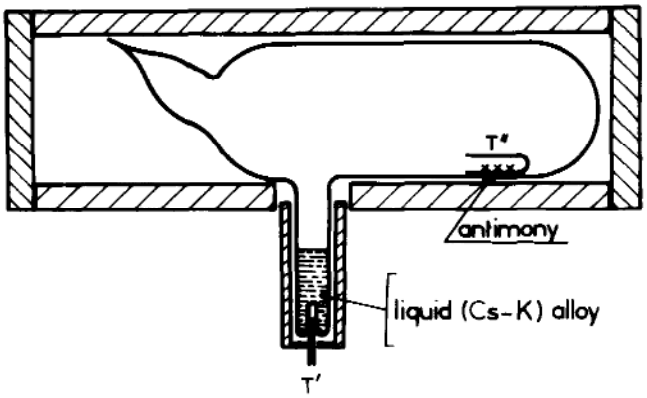

Fig. 2. Reactor and vapour generator used for the synthesis of bialkali antimonides.

These temperatures were chosen:

i) in the case of T″ by reference to industrial practice;

ii) for T′, in order to obtain acceptable kinetic conditions although avoiding an attack of the generator (pyrex glass) by the alkali metals.

It is worthwhile noting that the partial pressure of antimony at the reactor temperature ($\simeq 10^{-13}$ atm) was too low to induce an appreciable transport of this element towards the coldest parts of the apparatus. After the reaction, the apparatus was quickly cooled in air (≃5 min) in such a way that T″ was always maintained higher than T′ to avoid transfer of alkali elements towards the reactor.

Characterization of the phases obtained

Chemical analysis

The mass ratios of the alkali metals to antimony were determined from the weight gained by the antimony during the synthesis. The atomic ratios Cs/Sb were obtained from absorption spectrometry.

X-ray analysis

The composition of an unknown $(Cs_{1-x}Sb_x)_3Sb$ cubic phase can be obtained from its crystallographic parameter, a, provided the curve $a = f(x)$ is available.

Prior to the experiments described above, we determined this curve experimentally, using terms of the solid solution $(Cs_3Sb)_{1-x}(K_3Sb)_x$ obtained by direct combination, at 200 °C for 200 h, of a mixture of stoichiometric* Cs_3Sb and K_3Sb. The crystallographic parameter a was measured by the Debye-Scherrer technique, using the $K_{\alpha 1}$ radiation of copper. Several studies were made up to 200 °C in a Guinier-Simon chamber in order to check that no change in the nature of the phases occurred between 200 °C and room temperature.

The results obtained are summarized on Figs. 3 and 4. The solid solution extends from Cs_3Sb

*Whereas K_3Sb is a line compound, Cs_3Sb can exhibit departure from stoichiometry up to 1% as shown in an anterior study [7].

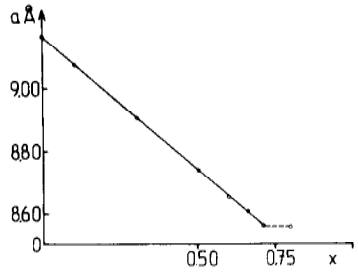

Fig. 3. Variation with x of the $(Cs_{1-x}K_x)_3Sb$ lattice parameter.

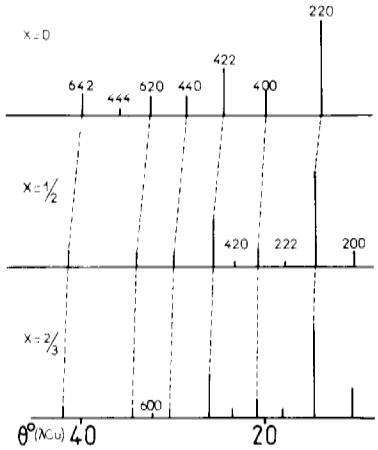

Fig. 4. Evolution with x of the $(Cs_{1-x}K_x)_3Sb$ X-ray diffraction pattern.

up to $(Cs_{0.29}K_{0.71})_3Sb$, *i.e.* $0 \leqslant x \leqslant 0.71$. A study of the intensities I_{hkl} of the lines such as $h+k+l=4n+2$ indicates that when cesium is substituted by potassium, the latter occupies preferentially the (c) sites in the lattice (see Fig. 1). For example, when $x=0.50$, the observed ratio I_{200}/I_{220} is approximately 12 when it should be close to 0.01 for a random occupation of (b) and (c) sites by the potassium atoms. As a matter of fact, all the (c) sites are occupied when $x=2/3$ as shown by McCarroll [5]. Since the solid solution extends beyond $x=2/3$, up to $x=0.71$, the (b) sites can then be occupied to an extent of 13%.

Results

The results obtained in systems A, B and C are represented on Fig. 5 with x (in $(Cs_{1-x}K_x)_3Sb$ as synthesized) as a function of the mole fraction X_K^L of potassium in the liquid mother K-Cs alloy.

As quoted before, K_3Sb is practically a line compound whereas Cs_3Sb can show significant departure from stoichiometry. Numerous analyses performed on the bialkali phases that we synthesized have shown that the ratio (K+Cs)/Sb can be slightly lower than 3 on the cesium rich side of the solid solution. The accuracy of our analytical

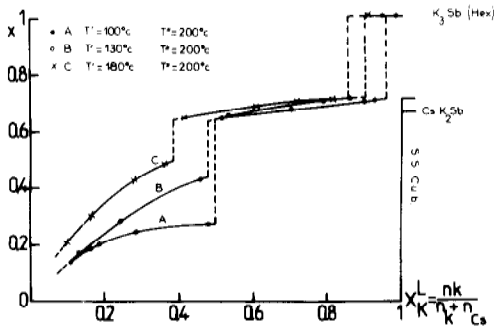

Fig. 5. Variation of the composition parameter x in $(Cs_{1-x}K_x)_3Sb$ as a function of the mole fraction K_K^L in the liquid mother alloy used for the synthesis of antimonides.

methods does not allow us to quantify such a deviation, which depends also on T′ and T″. It appears however that, whatever the values of T′ and T″, no significant deviation of (K+Cs)/Sb from the value 3 occurs when the mole fraction X_K^L of potassium in the mother alloy is higher than 0.1.

This corresponds to the nearly stoichiometric solutions $(Cs_{1-x}K_x)_3Sb$ with $x \geqslant 0.15$ which are then the object of the present study. The values of x in the phases that we synthesized have been determined by use of the curve in Fig. 3, after experimental measurement of their lattice parameter.

Measurements of the Seebeck coefficient for these phases lead in all cases to positive values showing then a slight deficit in alkali metals, although not detectable via chemical analysis. These results are in agreement with those of Fisher *et al.* [8] who found that the compound CsK_2Sb was a p-type conductor with a predominant intrinsic conductivity. All these results are also supported by the relatively weak thermionic emissivity of the corresponding photosensitive layers as compared to that of cesium excess $\simeq Cs_3Sb$: the high thermionic emissivity of the latter is attributed to its n-type character.

Thermodynamic interpretation

The bialkali antimonides are phases of variable composition and their synthesis can be easily interpreted by use of the formalism of solutions.

The Gibbs energy of formation of a given phase, starting from the pure elements, as it occurs in the reactor at T″ can be expressed as:

$$\Delta\bar{G} = X_{Cs}^S \Delta\bar{G}_{Cs} + X_K^S \Delta\bar{G}_K + X_{Sb}^S \Delta\bar{G}_{Sb} \qquad (1)$$

where X_i^S is the mole fraction of component i in the antimonide and:

$$\Delta\bar{G}_i = \bar{G}_i - G_i^0 \quad (3)$$

the difference between the molar Gibbs energy (or chemical potential) of i in the antimonide and in the reference state (*i.e.* pure condensed component) respectively.

In the antimonides, the activities are:

$$RT'' \ln a_i = \Delta\bar{G}_i \quad (3a)$$

$$\text{or } a_i = p_i/P_i^{\oplus} \quad (3b)$$

where P_i and $P_i^{\oplus}$ are the equilibrium pressure of i over the antimonide and over the reference state respectively, at temperature T''. Using pressures instead of fugacities is reasonable since the vapours considered behave practically as perfect gases.

The activities and chemical potentials of the three components in the antimonide synthesized at T'' can be fixed via the vapour pressures of the two alkali metals established at T' in the generator and which are:

$$P_i = \gamma_i^L X_i^L P_i^{\oplus} \quad (4)$$

where γ_i^L and X_i^L are respectively the activity coefficient and mole fraction of i in the mother alloy at T'. In such conditions the composition of the antimonide synthesized is defined. For every mother alloy composition used, the activities a_{Cs} and a_K in the antimonide synthesized can be obtained from relation (3b) and (4). Such values combined with a_{Sb} (obtained for example after integration of the Gibbs-Duhem equation) give access to the isothermal Gibbs energy – composition surface for the antimonides (surface Σ on Fig. 6). Use of such a surface to interpret phase equilibria [9] is explained under the figure caption.

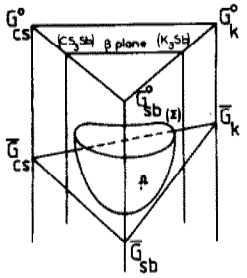

Fig. 6. Isothermal Gibbs energy-composition surface Σ for a phase of variable composition ϕ in a ternary system (Cs-K-Sb). Ω is the intersection of the vertical representing the composition of a ternary phase ϕ with the Gibbs energy-composition surface Σ. The plane tangent to Σ at point Ω intersects the verticals $X_{Cs}=1$, $X_K=1$ and $X_{Sb}=1$ at points or ordinates $\bar{G}_{Cs}$, $\bar{G}_K$ and $\bar{G}_{Sb}$ respectively (chemical potentials in ϕ).

When the two alkali chemical potentials are imposed via the vapour generator, this sets points of ordinates $\bar{G}_{Cs}$ and $\bar{G}_K$ through which only one plane tangent to Σ can be drawn. This plane intersects the vertical $X_{Sb}=1$ at point $\bar{G}_{Sb}$: the chemical potential of antimony and thus the composition of ϕ are then determined.

In practice, the limited variation of the ratio $X^S_{Cs}+X^S_K/X^S_{Sb}$ would lead to a large imprecision in the calculation of Σ via the Gibbs-Duhem integration. In practice, the curve σ, the intersection of Σ with the pseudo-binary plane Cs_3Sb-K_3Sb, can be used instead of Σ itself.

For such a practice we shall assume:

(i) that the Sb sublattice is little or not affected by the ratio Cs/K in the alkali sublattice

(ii) that $X^S_{Sb}\simeq 0.25$ and that consequently $\Delta\bar{G}_{Sb}$ is practically constant.

An alternative to the use of the σ curve is that of the partials $\ln a_{Cs}=f(X^S_{Cs})$ and $\ln a_K=f(X^S_K)$ as obtained from the experimental results.

Experimental curves ln $a_i=f(X_i)$

From relations (3b) and (4), the activities of i in the antimonides synthesized can be calculated through:

$$a_i^S = \gamma_i^L X_i^L \quad (5)$$

The activity coefficients γ_i^L in the mother liquid alloy are taken from Ciurylo and Rozwadowski [10] and the vapour pressures of the elements from Hultgren *et al.* [6]. Figure 7 shows the three curves obtained, which are relative to an unique reactor temperature (200 °C) and correspond to three generator temperatures (*i.e.* 100, 130, 180 °C). For every curve, whatever the generator temperature, three different domains appear within the composition range. We shall examine them successively.

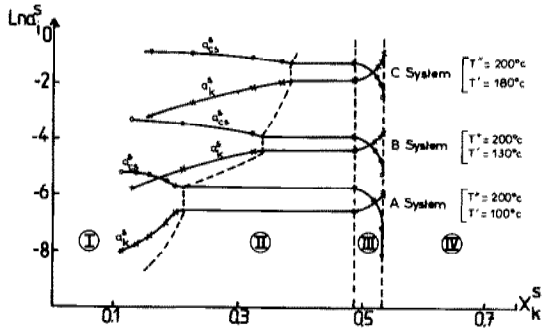

Fig. 7. Activity *versus* composition curves for alkali elements in bialkali antimonides at 200 °C; for various temperatures of the alkali generator.

Domain I

The composition of the phase synthesized varies regularly with that of the liquid mother alloy (see Fig. 5) and thus with the ratio a_{Cs}/a_K (Fig. 7). X-ray analysis indicates that these phases are cubic with a slight ordering of Cs and K between the alkali sublattices (b) and (c).

Domain II

In this domain, the composition of the phase synthesized varies sharply with the ratio a_{Cs}/a_K. Simultaneously order appears in the alkali sublattice (occupation of (b) sites by cesium and of (c) sites by potassium) giving rise to the peculiar CsK_2Sb structure.

Domain III

The composition of the phases synthesized varies very slowly with that of the liquid mother alloy and thus with the ratio a_{Cs}/a_K. The phases synthetized are in the composition range $Cs_{1.04}K_{1.96}Sb$-$Cs_{0.87}K_{2.13}Sb$ and structurally close to the ordered phase CsK_2Sb.

Isothermal Gibbs energy-composition curve

Indeed the system studied may be alkali deficient as we mentioned before. It should then be represented by a Σ surface. In that case the σ curve is generated by the set of points where the Σ surface is tangent to the successive planes containing the various couples of points ($\bar{G}_{Cs}$, $X_{Cs}=1$) and ($\bar{G}_K$, $X_K=1$), each of which corresponds to a liquid mother alloy composition. Of course, at a given generator temperature T', $\bar{G}_{Cs}$ and $\bar{G}_K$ are related via the Gibbs-Duhem equation. There is then a σ curve, on the isothermal (at T") Σ surface, for every generator temperature. Figure 8 shows such a curve semi qualitatively. It is worthwhile noting that in principle σ does not lie in the Cs_3Sb-K_3Sb pseudo-binary plane β. In practice, since the antimonides concerned are weakly alkali defective, any tangent to the plane curve σ drawn on Fig. 8 is very close to the intersection with β of the corresponding plane containing the points ($\bar{G}_{Cs}$, $X_{Cs}=1$), ($\bar{G}_K$, $X_K=1$) and tangent to Σ.

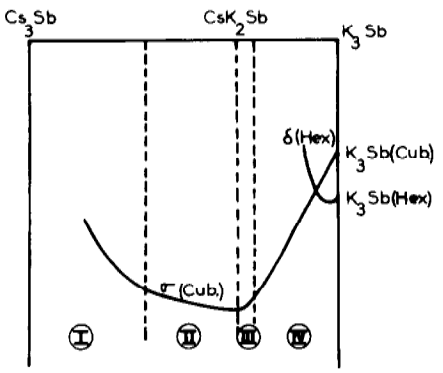

Fig. 8. Isothermal Gibbs-energy composition curves for nearly stoichiometric $(Cs_{1-x}K_x)_3Sb$ (*i.e.* nearly quasi binary system Cs_3Sb-K_3Sb).

For a given composition, the variation in the alkali ratio X^S_{Cs}/X^S_K resulting in a change in $\bar{G}_{Cs}$ and $\bar{G}_K$ (both related by the Gibbs-Duhem equation through the generator) depends on the radius of curvature of σ at the composition considered. If this radius is large, then a small variation in the alkali chemical potentials can induce drastic changes in the composition of the antimonide synthesized. On the contrary, in a domain where the radius of curvature is small, important variations in $\bar{G}_{Cs}$ and $\bar{G}_K$ will lead to antimonides with rather similar compositions.

Examining the curve in Fig. 8 can then provide guidance for the manufacturing of photoemissive bialkali antimonides, as was already suggested by the curves in Fig. 7 and the three domains mentioned there.

Domain I

The σ curve is nearly linear, which corresponds to a large radius of curvature: the composition of the phase synthesized is extremely sensitive to the ratio a_{Cs}/a_K. The same remark holds for the degree of ordering in the alkali sublattice.

Domain II

The radius of curvature of σ is smaller than in domain II. The composition of the slightly ordered phase obtained varies steadily with that of the liquid mother alloy composition.

Domain III

The radius of curvature of σ is very small. As a result, the composition of the ordered antimonide synthesized is not very sensitive to the ratio $a_{Cs}a_K$ (*i.e.* to the liquid mother alloy composition). This provides optimum conditions for a good reproducibility in the manufacturing of antimonides.

Examining Fig. 7 indicates that when the generator temperature is decreased, domain I decreases while domain II extends and domain III remains unchanged (Fig. 7). For a given reactor temperature, obtaining antimonides with compositions close to CsK_2Sb can then be achieved with a greater flexibility (*i.e.* broader authorized composition range for the liquid mother alloy) when the generator temperature is low.

Appearance of the hexagonal phase $\simeq K_3Sb$

Whatever the set up (T', T''), an hexagonal phase with composition $\simeq K_3Sb$ appears as soon as the ratio a_{Cs}/a_K exceeds its limiting value on the potassium rich side of domain III.

Thermodynamically, $\simeq K_3Sb$ must contain some cesium, but in an amount which lies beneath the limit sensitivity of our analytical method.

The sudden appearance of hexagonal $\simeq K_3Sb$ can be interpreted in terms of the relative position of the Gibbs energy surfaces for the cubic phases, Σ, and for the hexagonal phases, Δ. Intersections of these surfaces with the pseudo-binary plane Cs_3Sb-K_3Sb are represented in Fig. 8 as curves σ and δ respectively. In domain IV, the Δ surface shall correspond to low Gibbs energies. It shall then be the first one to be in contact with the plane containing points $\bar{G}_{Cs}, X_{Cs}=1$ and $\bar{G}_K, X_K=1$ when these points correspond to a ratio a_{Cs}/a_K which exceeds its limiting value on the potassium rich side of domain III.

Conclusions

The equilibria between antimonides $(Cs_{1-x}K_x)_3Sb$ and alkali vapour were studied at 200 °C, for various temperatures of the alkali vapour generator. The phases obtained are slightly alkali deficient especially when they are rich in cesium and also when their synthesis is achieved with a vapour generator set at a rather low temperature. As expected these antimonides are characterized by a p-type conductivity.

The best photoemissive properties are observed for the ordered compound CsK_2Sb. Our study shows that this compound is actually the end term of a solid solution, the ordering of which depends upon the composition, and thus processing parameters. The optimum conditions for a good reproductibility in the processing of photoemissive antimonides have been established for a temperature of 200 °C. Manufacturing photoemissive layers by equilibrating the antimonides with binary alkali vapours would lead to a product with a better definition than those obtained through the dynamic process used at present.

References

1 A. H. Sommer, *Photoemissive Materials,* Wiley, 1968, pp. 56–131.
2 G. Gnutzmann, *Ph.D. Thesis, University of Munich,* 1953.
3 A. A. Dowman, T. H. Jones and A. H. Beck, *J. Phys. D: Appl. Phys., V8* (1975) 69.
4 G. Brauer and E. Zintl, *Z. Phys. Chem., B37* (1937) 323.
5 W. H. McCarroll, *J. Phys. Chem. Solids, 26* (1965) 191.
6 R. Hultgren, P. D. Desai, D. T. Hawkins, M. Gleiser, K. K. Kelley and D. D. Wagman, *Selected Values of Thermodynamic Properties of Elements,* A.S.M. Metals Park, Ohio, 1973.
7 J. M. Barois, C. Fouassier, M. Onillon and B. Tanguy, *Mater. Chem. Phys., 24* (1989) 189.
8 M. G. Fisher, A. F. McDonie and A. H. Sommer, *J. Appl. Phys., V45* (1974) 487.
9 M. Onillon, *J. Mater. Educ., 8* (1986) 305.
10 J. Ciurylo and M. Rozwadowski, *Acta Phys. Pol., A51* (1977) 583.